Source Signatures of Fine Particulate Matter from Petroleum Refining and Fuel Use

DOE Award No.: DE-AC26-99BC15220—01

Semi-Annual Report
Start Date: 07/01/1999 End Date: 01/31/2000

Consortium for Fossil Fuel Liquefaction
533 South Limestone Street Room 111
University of Kentucky
Lexington, KY 40506

Characterization of Fine Particulate Matter Produced by Combustion of Residual Fuel Oil

Gerald P. Huffman, Frank E. Huggins, Naresh Shah, and Robert Huggins,

University of Kentucky, CFFLS, 533 S. Limestone St. – Rm.111, Lexington, KY 40506

William P. Linak and C. Andrew Miller, U.S. Environmental Protection Agency, National Risk Management Research Laboratory, Research Triangle Park, NC 27711

Ronald J. Pugmire and Henk L. C. Meuzelaar,

Dept. of Chemical and Fuels Engineering, University of Utah, Salt Lake City, UT 84112

Mohindar S. Seehra and A. Manivannan

Physics Department, West Virginia University, Morgantown, WV 26506

ABSTRACT

Combustion experiments were carried out on four different residual fuel oils in a 732 kW boiler. Particulate matter (PM) emission samples were separated aerodynamically by a cyclone into fractions that were nominally less than and greater than 2.5 microns in diameter. However, examination of several of the samples by computer-controlled scanning electron microscopy (CCSEM) revealed that part of the <2.5 micron fraction ($PM_{2.5}$) in fact consists of carbonaceous cenospheres and vesicular particles that range up to 10 microns in diameter. X-ray absorption fine structure (XAFS) spectroscopy data were obtained at the S, V, Ni, Fe, Cu, Zn, and As K-edges, and at the Pb L-edge. Deconvolution of the x-ray absorption near edge structure (XANES) region of the S spectra established that the dominant molecular forms of S present were sulfate (26-84% of total S) and thiophene (13-39% of total S). Sulfate was greater in the $PM_{2.5}$ samples than in the >2.5 micron samples ($PM_{2.5+}$). Inorganic sulfides and elemental sulfur

were present in lower percentages. The Ni XANES spectra from all of the samples agree fairly well with that of $NiSO_4$, while most of the V spectra closely resemble that of vanadyl sulfate ($VO•SO_4•xH_2O$). The other metals investigated (Fe, Cu, Zn, and Pb) were also present predominantly as sulfates. Arsenic is present as an arsenate (As^{+5}). X-ray diffraction patterns of the $PM_{2.5}$ fraction exhibit sharp lines due to sulfate compounds (Zn, V, Ni, Ca, etc.) superimposed on broad peaks due to amorphous carbons. All of the samples contain a significant organic component, with the LOI ranging from 64 to 87 % for the $PM_{2.5}$ fraction and from 88 to 97% for the $PM_{2.5+}$ fraction. ^{13}C nuclear magnetic resonance (NMR) analysis indicates that the carbon is predominantly condensed in graphitic structures. Aliphatic structure was detected in only one of seven samples examined.

IMPLICATIONS

Regulations on $PM_{2.5}$ should be based on the best scientific data, particularly with regard to characterization. Although there are many analytical techniques for determining the elemental composition of $PM_{2.5}$, information on molecular structure and microstructure is difficult to obtain. The current paper presents the results of an investigation of the structure of $PM_{2.5}$ from combustion of residual oil using a variety of analytical techniques (XAFS spectroscopy, CCSEM, ^{13}C NMR, ICP/MS and XRD). The results demonstrate that these techniques provide a rather complete analysis of the molecular structure of both the inorganic and organic components of the $PM_{2.5}$. Improved information is also obtained on particle size distributions, composition ranges, and morphologies. Since both health effects and source apportionment of $PM_{2.5}$ are closely related to such parameters, this type of information should be valuable to regulatory authorities and to industry.

INTRODUCTION

The U.S. Environmental Protection Agency (EPA) is currently considering new regulations for fine airborne particulate matter (PM) less than 2.5 microns in diameter ($PM_{2.5}$). Such regulations should be based on the best scientific data, particularly with regard to fine particle characterization. Although there are many analytical techniques for determining the elemental composition of $PM_{2.5}$, there has been relatively little research on its molecular structure and microstructure. Many scientists believe that both the effects on human health and the source apportionment of $PM_{2.5}$ are closely related to parameters such as particle size distributions and morphology, and the valence and solubility of critical elements. It is therefore essential to identify and evaluate analytical methods that can provide such structural information.

X-ray absorption fine structure (XAFS) spectroscopy is a synchrotron radiation – based technique that is uniquely well suited to characterization of the molecular structure of individual elements in complex materials. In previous research, we have used XAFS spectroscopy to determine the molecular forms of environmentally important elements (S, Cl, As, Cr, Hg, Ni, etc.) in coal, oil, flyash, and sorbents.[1-7] Our initial investigations of PM indicate that XAFS will also be a powerful tool in this area.[8,9]

In the current work, XAFS spectroscopy and a number of additional analytical techniques were applied to a suite of residual oil flyash (ROFA) samples separated aerodynamically into $PM_{2.5}$ and $PM_{2.5+}$ fractions. Briefly, the characterization data obtained included:

1. XAFS analysis of the molecular structure of S, V, Ni, Fe, Cu, Zn, Pb, and As.
2. Computer-controlled scanning electron microscopy (CCSEM) analysis of particle size, composition, and morphology.

3. ^{13}C nuclear magnetic resonance (NMR) analysis of the molecular structure of carbon, the dominant element.
4. X-ray diffraction (XRD) identification of crystalline phases.
5. Inductively coupled plasma - mass spectrometry (ICP-MS) determination of metal concentrations.

A summary of the information obtained from these measurements is presented below.

COMBUSTION PROCEDURE

The combustion experiments were carried out in a North American three-pass fire tube package boiler, which is a practical, commercially available heavy fuel oil combustion unit. A detailed description of this boiler is given elsewhere.[10] Samples were separated aerodynamically by a cyclone into $PM_{2.5}$ and $PM_{2.5+}$ fractions. The sampling system consists of a large dilution sampler capable of isokinetically sampling 0.28 m^3/min (10 ft^3/min) of flue gas using a Source Assessment Sampling System (SASS) cyclone. Details on the construction and operation of this sampling system are available elsewhere.[11] The SASS cyclone produces 50 and 95% collection efficiencies at approximately 1.8 and 2.5 micron diameter, respectively. The resulting PM is collected on large (65 cm) Teflon-coated glass fiber filters, transferred to sampling jars, and made available for analysis.

Four residual fuel oils were combusted, with sulfur contents ranging from 0.53 to 2.33 wt. %. The ultimate analyses of these oils, together with the concentrations of the metals of interest for this paper, are given in Table 1. Table 2 contains the loss on ignition (LOI) and metal concentrations for the $PM_{2.5}$ and $PM_{2.5+}$ fractions. The metal analyses were performed using acid digestion and inductively coupled plasma mass spectrometry (ICP-MS).[10] Although

burnout was fairly complete (>99.7 %), the inorganic content of the oils was quite low (0.02-0.10 wt.% ash), and the LOI results indicate that the dominant element of the ROFA is carbon (64-87 wt.% for $PM_{2.5}$ and 88-97 wt.% for $PM_{2.5+}$). V is present at relatively large concentrations (~0.5-5 wt. %), Ni, Fe and Zn at moderate concentrations (~0.1-0.5 wt.%), and several metals (Pb, As, Cr, Cu, Mn, Sb, and Cd) at concentrations that are rather low (~20 ppm-1000 ppm), but could still be significant for health considerations. The metals are typically more concentrated in the $PM_{2.5}$ samples than in the $PM_{2.5+}$ samples by factors ~3 to 6.

XAFS SPECTROSCOPY RESULTS

The samples were investigated by XAFS spectroscopy at the Stanford Synchrotron Radiation Laboratory (SSRL) and the National Synchrotron Light Source (NSLS) at Brookhaven National Laboratory. All measurements were carried out in the fluorescent mode using either a Lytle detector or a multi-element Ge array detector, as described elsewhere.[1-4] The XANES regions of the spectra were analyzed by deconvolution, derivative, and comparative analysis methods, as discussed in earlier papers.[1-7] The results for the elements investigated to date are summarized below.

Sulfur: Typical S K-edge XANES spectra of ROFA $PM_{2.5}$ and $PM_{2.5+}$ samples are shown in Figure 1. The spectra are deconvoluted by a least squares computer analysis into a series of peaks (50% Lorentzian-50% Gaussian) and two rounded arctangent step functions, as discussed elsewhere.[1,2] Most of the peaks represent 1s→3p transitions of photoelectrons excited from the K-shell by x-ray absorption. Both the position and relative intensity of these peaks vary significantly with the electronic state of the S atom, increasing with increasing valence. By using calibration data generated from mixtures of standard compounds, the peak area

percentages can be translated into percentages of the total S contained in different molecular forms.[1,2]

The results of this analysis for the ROFA PM samples are summarized in Table 3. The dominant molecular forms of S observed are sulfate and thiophenic S. Sulfate was greater in the $PM_{2.5}$ samples than in the $PM_{2.5+}$ samples, reflecting the greater degree of carbon burnout for the smaller particles. Additional components, including elemental S and inorganic sulfides, are present in lower percentages. The origin of the elemental S is not clear at this time. The S in the $PM_{2.5}$ of the ROFA from a high S residual oil burned in a second furnace where carbon burnout was much more complete was 100% sulfate.

Vanadium: The molecular forms of the metals investigated in this study were identified by comparing the XANES spectra and the first derivative of the XANES spectra of the ROFA samples to those of standard compounds. The standard compound suite included most of the oxides, sulfates, and sulfides of each metal investigated.

Most of the V XANES and first derivative XANES spectra from both the $PM_{2.5}$ and $PM_{2.5+}$ fractions closely resemble the spectrum of vanadyl sulfate ($VO{\bullet}SO_4{\bullet}xH_2O$). This is brought out most clearly by the distinctive first derivative of the XANES spectrum, which exhibits peaks in nearly identical positions and with similar intensities to the first derivative of the XANES spectrum of $VOSO_4{\bullet}3H_2O$ reported by Wong et al.[12] and also measured by our group in this study. Typical V XANES and first derivative spectra from a $PM_{2.5}$ sample are shown in Figure 2. The spectra of several samples also indicate the presence of minor amounts of oxide, probably V_2O_5.

Nickel: The Ni XANES and first derivative spectra from the PM samples (Figure 3) were found to agree well with those of $NiSO_4$. For ease of comparison, the absorption scale for

all spectra has been normalized to the same arbitrary unit of intensity. Similar XAFS results were obtained for Ni in an earlier investigation of ROFA[5] by the current authors. There is again evidence of a small amount of oxide (NiO) in one of the $PM_{2.5}$ samples (low S No. 6), both in the first derivative spectrum and the radial structure function obtained by Fourier analysis of the XAFS spectrum.

Iron: The Fe XANES and the first derivatives of the Fe XANES of the ROFA PM samples (Figure 4) agree well with those of ferric sulfate, $Fe_2(SO_4)_3$, indicating that it is the dominant iron compound in both the $PM_{2.5}$ and $PM_{2.5+}$ samples. This conclusion was reached by comparing the spectra for the ROFA PM samples with those of numerous iron-based standard compounds. One $PM_{2.5}$ sample (low S No. 6) contains a small amount of iron oxide, probably Fe_3O_4.

Copper, zinc, and lead: Although fewer samples have been examined and the data are of somewhat lower quality because of lower concentrations, it appears that sulfates are the dominant phases detected by the XANES spectra for these metals also. The phases tentatively identified are $CuSO_4 \cdot xH_2O$, $ZnSO_4$, and $PbSO_4$.

Arsenic: The As XANES spectra establish that the arsenic is present as an arsenate (As^{+5}) but do not identify the specific phase. A discussion of the identification of arsenic valence states from XANES spectra can be found in references 3 and 4.

CCSEM DATA

The principles of CCSEM have been summarized in numerous previous papers. Briefly, as the electron beam is rastered across the sample, the back-scattered electron intensity is measured and compared to a preset discriminator level to detect particles. When a particle is detected, the

stepping density of the electron beam is increased by a factor of 256 and the cross-sectional area, maximum and minimum diameters, and energy dispersive x-ray (EDX) spectrum of the particle are measured. Details of the measurement procedure are summarized elsewhere.[13-15] With a well prepared sample, it is possible to measure the size and approximate composition of ~ 1000 particles in several hours. In the current studies, the CCSEM examination was carried out on PM samples dispersed on nucleopore filters, prepared as discussed elsewhere.[13] For the current PM samples, C was by far the dominant element detected in the EDX spectra, while S was detected in most particles at concentrations ~1-10%. Since EDX collection times were only 5 sec per particle, V, Ni and other metals were detected only as minor components of selected particles.

Some preliminary CCSEM data for two ROFA $PM_{2.5}$ samples are shown in Table 4 and Figure 5. The data are considered to be preliminary at this point because preparation of satisfactory SEM specimens for these samples has proven to be difficult and we are still refining our procedures. Consequently, the current data, while informative, should be considered qualitative in nature. Table 4 indicates the three major classes of particles identified and the average composition of those classes based on the EDX spectra. Better information can be obtained regarding particle composition by the use of binary and ternary composition diagrams,[13] such as the C - S diagram for the medium S No. 6 $PM_{2.5}$ sample shown in Figure 5a. This diagram includes all particles for which C + S was >80%. It illustrates that the carbon-rich char particles contain a range of S concentrations, from 0 to approximately 20%, with peaks in the 0-2 and the 6-10% ranges. The particle size distribution (PSD) for all of the particles analyzed for the low S #6 $PM_{2.5}$ sample is shown in Figure 5b. It is seen that a significant percentage of the particles classified aerodynamically as $PM_{2.5}$ by the cyclone separator are in fact >2.5 microns in diameter. Many of these appear to be cenospherical, vesicular, carbon

particles, such as those shown in Figure 6. The arrows in Figure 6 indicate inorganic particles rich in V and S, some of which also contain Ca, Al and Si. These particles presumably consist primarily of vanadyl sulfate. It is worth noting that this type of configuration, small particle transition metal phases on a highly porous carbon support, could act as a good catalyst for chemical reactions. This type of microstructure is frequently observed in the ROFA $PM_{2.5}$.

NMR DATA

^{13}C NMR has been used extensively to examine the molecular structure of carbon in a wide range of materials. It is perhaps the best method of measuring the relative percentages of aromatic and aliphatic carbon in organic materials and can provide detailed information on the extended carbon skeletal structure and bonding groups. Detailed discussion of the methodology involved in such analyses is given elsewhere.(16) Four of the $PM_{2.5}$ and three of the $PM_{2.5+}$ ROFA samples were examined by ^{13}C NMR. Cross polarization experiments suggested that the proton content of the samples was very low and, hence, no useful data were obtained using this experimental technique. Proton spectra taken on several samples verified the very low H/C ratios for all but the $PM_{2.5}$ sample derived from combustion of the high sulfur No.6 oil. The ^{13}C NMR spectra were then acquired by using block decay with a pulse repetition rate of 10 s and accumulating between 17,000 and 25,000 scans. Six of the seven samples examined exhibited spectra essentially identical to that shown in Figure 7 for the low S No. 6 oil $PM_{2.5}$ sample. These spectra indicate that the carbon in these samples is predominantly condensed in graphitic structures. Second moment (line width) measurements are uniform at ~75 ppm (full width at half height - FW/HH) for all six of the samples. However, the second moment for the high sulfur

high S No. 6 $PM_{2.5}$ sample indicates a much narrower aromatic band (peak at ~120 ppm, FW/HH = 45 ppm) and the spectrum clearly shows the presence of aliphatic structure (peak at ~20ppm).

XRD DATA

The x-ray diffraction (XRD) experiments were carried out using a Wide Angle X-Ray Diffractometer (Rigaku Model D/Max) employing CuKα radiation (λ = 1.5418 Å). The data were taken in the step-scan mode using 0.04° steps and 30 sec collection time at each step. The data was analyzed using a Jade software package and the JCPDS data files.

Typical x-ray diffractograms are shown in Figure 8 for the $PM_{2.5}$ from the No. 5 oil and the $PM_{2.5}$ and $PM_{2.5+}$ from the high S No. 6 oil. The diffractograms consist of sharp lines superposed on two broad peaks at 2θ = 26° and 44°. The broad peaks are due to amorphous carbon[17]. The sharp lines are due to inorganic compounds and have been identified as sulfates and sulfites of Zn, V, Ni, Pb, Fe, Ca, and Cu. The identified compounds are: $CaSO_4$, $Zn_4SO_4(OH)_6 \cdot 5H_2O$, $Zn(SO_3)2.5H_2O$, $VOSO_4$, $NiSO_4 \cdot 6H_2O$, PbS_2O_3, $Fe_3(SO_4)_4 \cdot 14H_2O$, $ZnSO_4 \cdot xH_2O$, $Ca(SO_4) \cdot 2H_2O$, Cu_2SO_4. Qualitatively, the intensities of the lines is the largest for samples obtained from the high sulfur No. 6 oil and for the $PM_{2.5}$ fraction of No. 5 oil (BL5FH). This is understandable since the high sulfur content would tend to produce higher levels of the sulfates. Generally, $PM_{2.5}$ fractions tend to have higher concentrations of the sulfates as compared to the $PM_{2.5+}$ fractions, as illustrated by the comparison of the diffractograms for the $PM_{2.5}$ and $PM_{2.5+}$ fractions from high sulfur No. 6 oil in Figure 8. For the $PM_{2.5}$ fraction from the No. 5 oil, the intensities of the lines are the largest of all the samples, but only weak lines due to $CaSO_4$ are observed for the $PM_{2.5+}$ fraction. A more complete summary of all the XRD data has been given elsewhere.[18]

SUMMARY AND CONCLUSIONS

The structure of $PM_{2.5}$ and $PM_{2.5+}$ from the combustion of several residual fuel oils in a commercial boiler has been characterized by a range of analytical techniques. XAFS spectroscopy was used to investigate the molecular structure of S, a number of metals (V, Ni, Fe, Zn, Cu, and Pb) and As. Deconvolution of the S XANES spectra revealed that the dominant molecular forms of S observed were sulfate and thiophenic S. Sulfate was greater in the $PM_{2.5}$ samples than in the $PM_{2.5+}$ samples, reflecting the greater degree of carbon burnout for the smaller particles. Sulfates were identified by XAFS as the dominant metal compounds [$VOSO_4 \cdot xH_2O$, $NiSO_4$, $Fe_2(SO_4)_3$, etc]. Arsenic was present as an arsenate (As^{+5}). XRD also identified a number of metal sulfates and sulfites, including $CaSO_4$. CCSEM measurement of the particle size distributions of two $PM_{2.5}$ samples established that a significant percentage of particles exceeded 2.5 microns in diameter. Many of these were vesicular, cenospherical, carbon char particles. The surfaces of these highly porous carbon particles were decorated with small (~1-3 micron) metal sulfate particles. ^{13}C NMR indicated that the carbon in the PM was predominantly graphitic or soot-like in structure, with only one sample exhibiting an aliphatic component.

The current study is part of a more general investigation of petroleum-derived $PM_{2.5}$. Future work, in addition to further characterization of the current samples, will include characterization of diesel emissions and PM samples collected on filters from the ambient atmosphere in appropriate locations.

Acknowledgement: Support of this research under U.S. Department of Energy (FE/NPTO) contract No. DE-AC26-99BC15220 is gratefully acknowledged. The XAFS experiments were conducted at the Stanford Synchrotron Radiation Laboratory and the National Synchrotron Light Source, which are also supported by the U.S. DOE.

References:

1. G.P. Huffman, S. Mitra, F.E. Huggins, N. Shah, S.Vaidya, and F. Lu, **1991**, *Energy & Fuels*, **5**, 574-581.
2. M.Mehdi Taghiei, F.E. Huggins, N. Shah, and G.P. Huffman, **1992**, *Energy & Fuels*, **6**, 293-300.
3. G.P. Huffman, F.E. Huggins, N. Shah, and J. Zhao, **1994**, *Fuel Processing Technology*, **39**, 47-62.
4. F.E. Huggins and G.P. Huffman, **1996**, *Int. J. Coal Geology*, **32**, 31-53.
5. K.C. Galbreath, C.J. Zygarlicke, D.L. Toman, F.E. Huggins, and G.P. Huffman, **1998**, *Energy & Fuels*, **12(4)**, 818-822.
6. F.E. Huggins, M. Najih, and G.P. Huffman, **1999**, *Fuel*, **78**, 233-242.
7. F.E. Huggins, G. P. Huffman, G. E. Dunham, and C. L. Senior, **1999**, *Energy & Fuels*, **13**, 114-121.
8. F.E. Huggins, G.P. Huffman, and J. David Robertson, ACS, Div. Environ. Chem., Preprints, 1998, **38(2)**.
9. F. E. Huggins and G. P. Huffman, **1999**, *J. of Hazardous Materials*, in press.
10. C. A. Miller, W. P. Linak, C. King, and J. O. L. Wendt, **1998**, *Combust. Sci. and Technol*., **134**, 477-502.

11. W.J. Steele, A.D. Williamson, and J.D. McCain, **1988**, Construction and operation of 10 cfm sampling system with a 10:1 dilution ratio for measuring condensable emissions, EPA/600-8-88-069 (NTIS PB88-198551), Research Triangle Park, NC, April.

12. J. Wong, F.W. Lytle, R.P. Messmer, and D.H. Maylotte, **1984**, *Phys. Rev. B*, **30**, 5596-5610.

13. G. Huffman, A. Shah, N. Shah, J. Zhao, F. Huggins, J. Helble, S. Srinivasachar, T. Peterson, J. Wendt, N. Gallagher, L. Bool, and A. Sarofim, Proc. Eng. Fd. Conf., The Impact of Ash Deposition on Coal Fired Plants, Eds., J. Williamson and F. Wigley, **1994**, pp. 409-423, Taylor & Francis, London.

14. F. E. Huggins, D. A. Kosmack, G. P. Huffman, and R. J. Lee, "Coal Mineralogies by SEM Automatic Image Analysis," **1980,** *Scanning Electron Microscopy*, Vol. I, 531-540, SEM Inc., AMF O'Hare, Chicago, IL 60666, USA.

15. G. P. Huffman, F. E. Huggins, and N. Shah, **1990**, *Progress in Energy and Combustion Science*, **16**, #4, 293-302.

16. M. S. Solum, R. J. Pugmire, and D. M. Grant, **1989**, *Energy & Fuels*, **3**, 187-193.

17. V. S. Babu, L. Farinash and M. S. Seehra, J. Mater. Res. 10, 1075 (1995).

18. A. Manivannan and M. S. Seehra, ACS Fuel Division Preprints (in press).

Table 1. Analysis of the four fuel oils examined.

	No. 5 oil	Low sulfur No. 6 oil	Medium sulfur No. 6 oil	High sulfur No. 6 oil
Ultimate Analysis, wt.%				
Carbon	86.36	86.00	86.48	85.49
Hydrogen	10.82	11.29	10.98	10.36
Nitrogen	0.33	0.43	0.43	0.35
Sulfur	1.73	0.53	0.93	2.33
Oxygen*	0.34	1.24	0.67	0.92
Moisture	0.35	0.50	0.50	0.50
Ash	0.07	0.02	0.03	0.10
Elemental Analysis, mg/g				
Arsenic	2	0.2	0.2	0.1
Beryllium	<1	<0.3	<0.3	<0.3
Cadmium	0.1	0.50	0.60	0.60
Chromium	0.5	1.08	0.96	1.05
Copper	4	0.56	0.78	3.5
Iron	50	23	19	21
Lead	3	0.80	0.58	4.5
Mercury	-	0.06	0.12	0.10
Nickel	34	17	22	30
Selenium	<2	<0.1	<0.1	<0.1
Vanadium	180	35	70	220
Zinc	39	4.11	3.70	74

* Determined by difference.

Table 2. Metal concentrations and enrichment ratios of $PM_{2.5}$ and $PM_{2.5+}$ samples (mg/g).

	Low sulfur No. 6 oil			Medium sulfur No. 6 oil			High sulfur No. 6 oil			No. 5 oil		
	2.5	2.5+	2.5/2.5+	2.5	2.5+	2.5/2.5+	2.5	2.5+	2.5/2.5+	2.5	2.5+	2.5/2.5+
Antimony	23.4	4.90	4.8	24.2	2.9	8.3	48.6	8.20	5.9	34.5	4.86	7.1
Arsenic	49.9	11.0	4.5	49.8	4.9	10	35.9	8.60	4.2	18.7	1.70	11
Beryllium	0.40	0.10	4.0	0.47	0.11	4.3	0.46	0.15	3.1	0.44	0.20	2.2
Cadmium	0.50	0.21	2.4	1.26	0.46	2.7	19.3	1.84	11	2.75	0.69	4.0
Chromium	32.6	27.5	1.2	44.7	46.9	1.0	60.2	41.3	1.5	60.5	33.3	1.8
Copper	123	33.8	3.6	159	36.8	4.3	1050	222	4.7	233	58.1	4.0
Iron	5100	1410	3.6	4460	1510	3.0	3850	2300	1.7	4220	1110	3.8
Lead	114	21.5	5.3	164	22.4	7.3	990	94.2	11	-	-	-
Magnesium	1450	428	3.4	1450	436	3.3	6190	2220	2.9	1770	101	18
Manganese	93.3	34.1	2.7	84.5	37.1	2.3	73.2	42.8	1.7	89.9	23.6	3.8
Nickel	4840	863	5.6	7470	1230	6.1	8020	2270	3.5	10600	2200	4.8
Vanadium	14700	4510	3.2	35300	7560	4.7	58900	19900	3.0	58600	13000	4.5
Zinc	1600	328	4.9	1840	422	4.4	21000	2740	7.7	2750	6530	0.4
LOI, mg/g	658	903	0.7	790	978	0.8	866	969	0.9	641	883	0.7

Table 3. XANES results for the percentages of the total sulfur contained in different molecular forms in ROFA PM samples.

Sample	PM size (micron)	Sulfate	Thiophene	Elemental S	Inorganic sulfide	Other forms
# 5 oil	< 2.5	55	24	5	11	5
# 5 oil	>2.5	32	37	8	19	4
Low S #6 oil	< 2.5	84	14	--	--	2
Low S #6 oil	>2.5	58	34	6	--	2
Med. S #6 oil	< 2.5	73	13	6	--	8
Med. S #6 oil	>2.5	55	35	6	--	3
High S #6 oil	< 2.5	54	29	5	11	1
High S #6 oil	>2.5	26	39	9	26	--

Table 4. CCSEM results for two $PM_{2.5}$ samples. Composition in atomic %.

Medium S # 6 $PM_{2.5}$ - 689 particles.						
Classes	Number	Number %	C	S	Al	Si
C/S rich	423	61.4	83	10	1	1
C rich	222	32.0	94	2	1	1
Al/Si rich	35	5.3	59	2	11	26
Others	9	1.3				

Low S # 6 $PM_{2.5}$ - 522 particles.						
Classes	Number	Number %	C	S	Al	Si
C/S rich	310	58.4	82	11	1	1
C rich	177	36.7	94	1	2	0
Al/Si rich	20	3.6	60	4	12	21
Others	15	1.3				

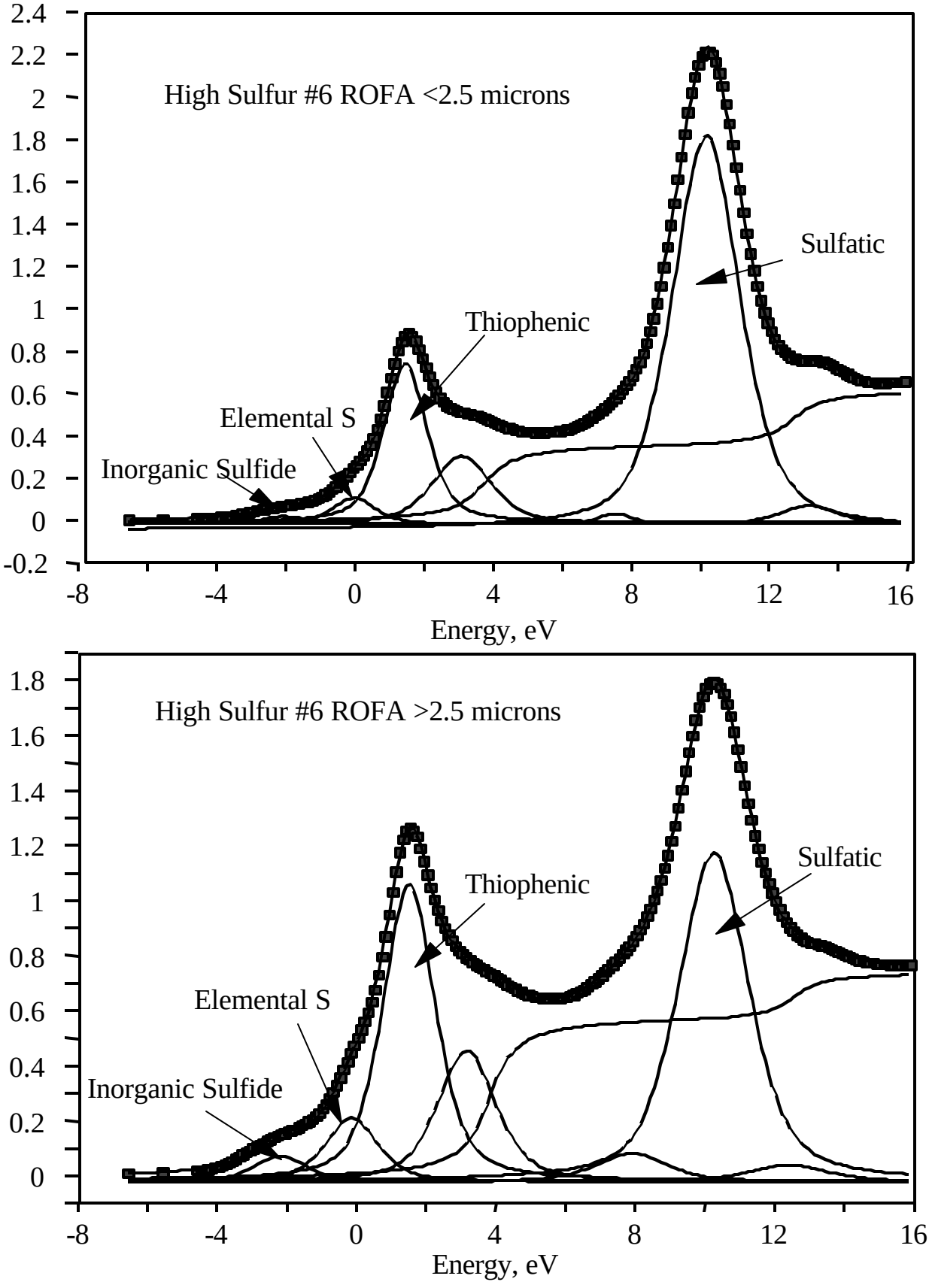

Figure 1. Typical deconvolution of S K-edge XANES spectra of ROFA $PM_{2.5}$ and $PM_{2.5+}$.

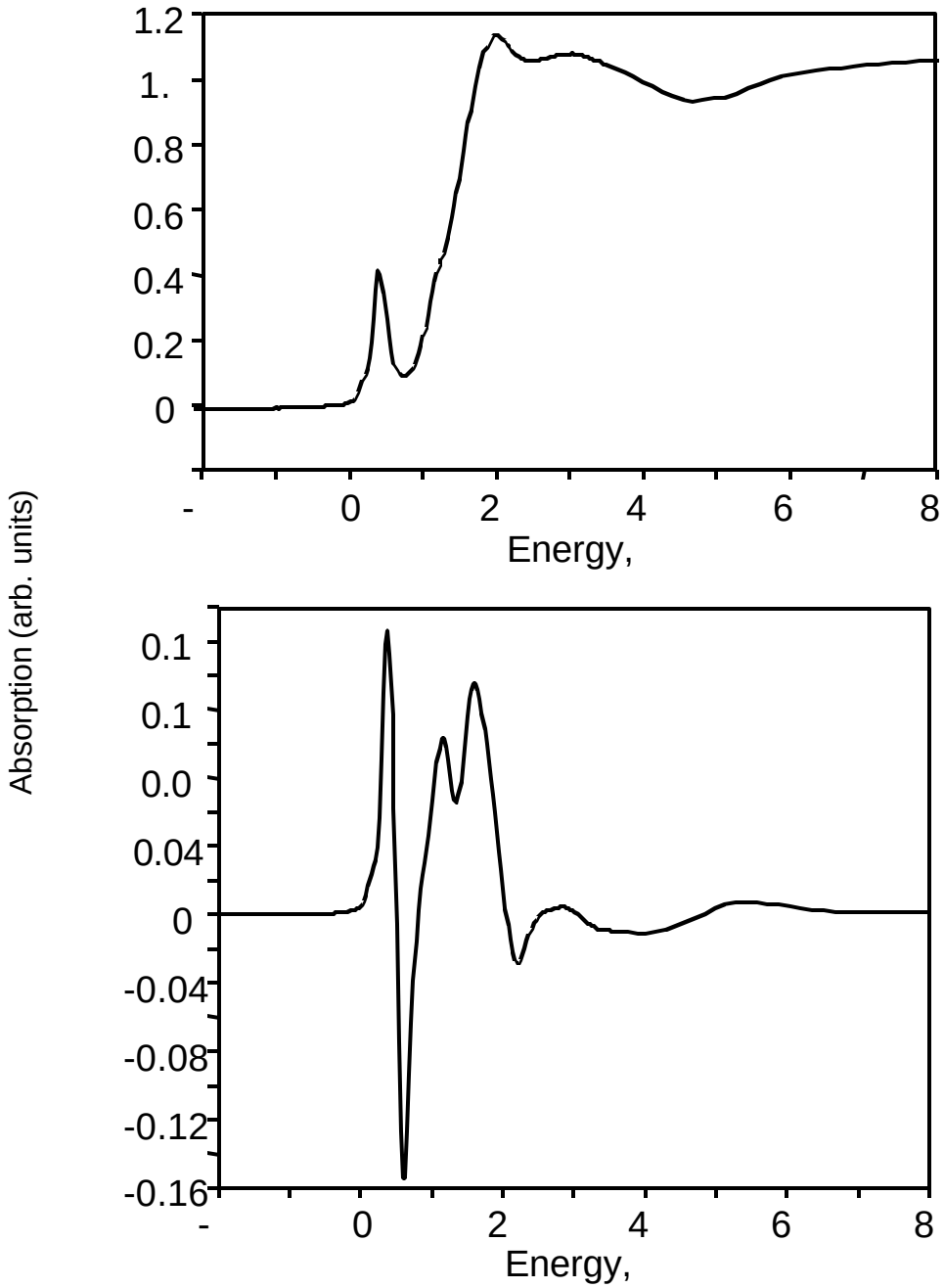

Figure 2. Distinctive V K-edge XANES (top) and first derivative spectra for the ROFA PM2.5 samples identify vanadyl sulfate ($VOSO_4 \cdot xH_2O$) as the dominant molecular form of vanadium.

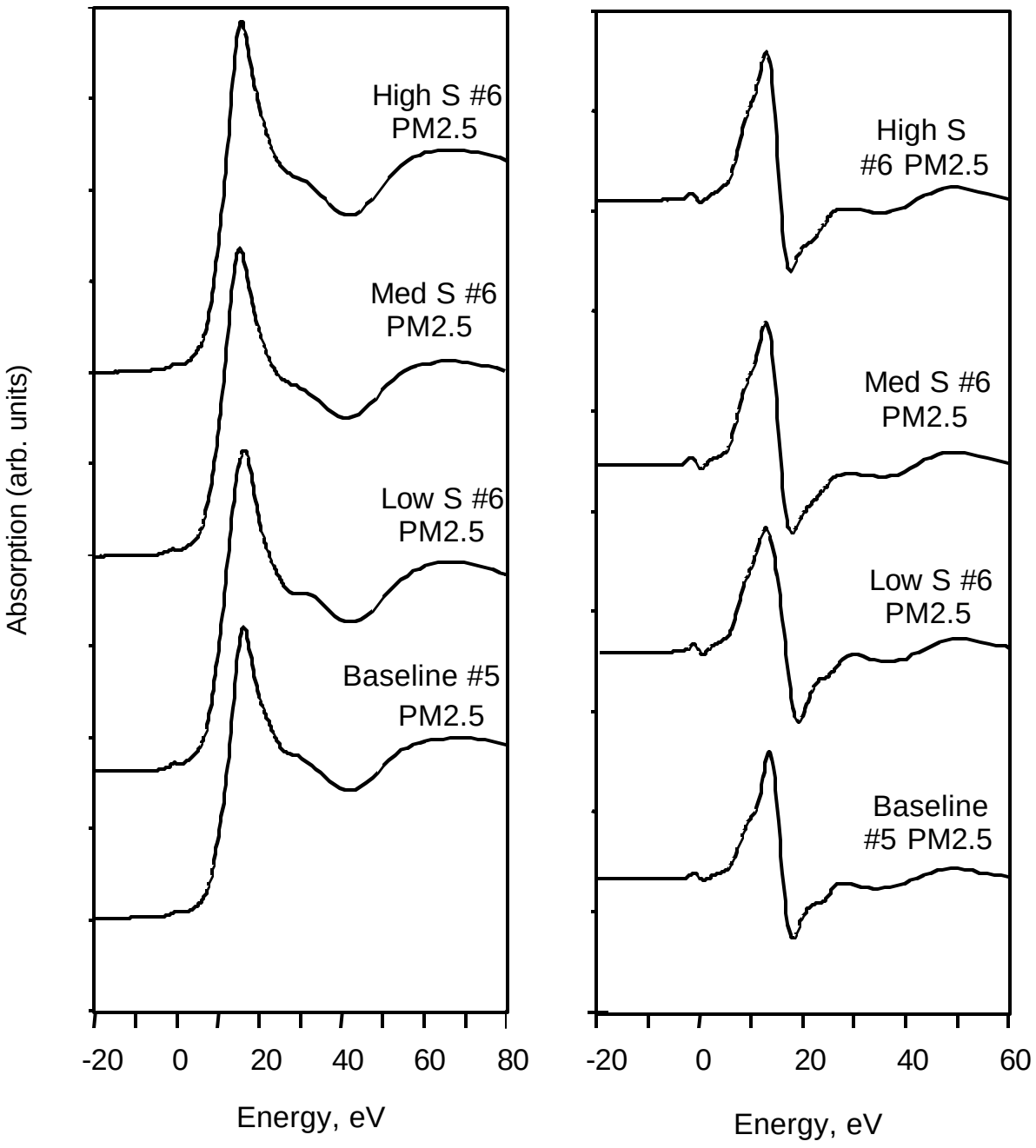

Figure 3. Ni XANES and first derivative spectra for the ROFA PM2.5 indicate that the dominant Ni phase is $NiSO_4$. The spectra are normalized to unit step height for easy comparison.

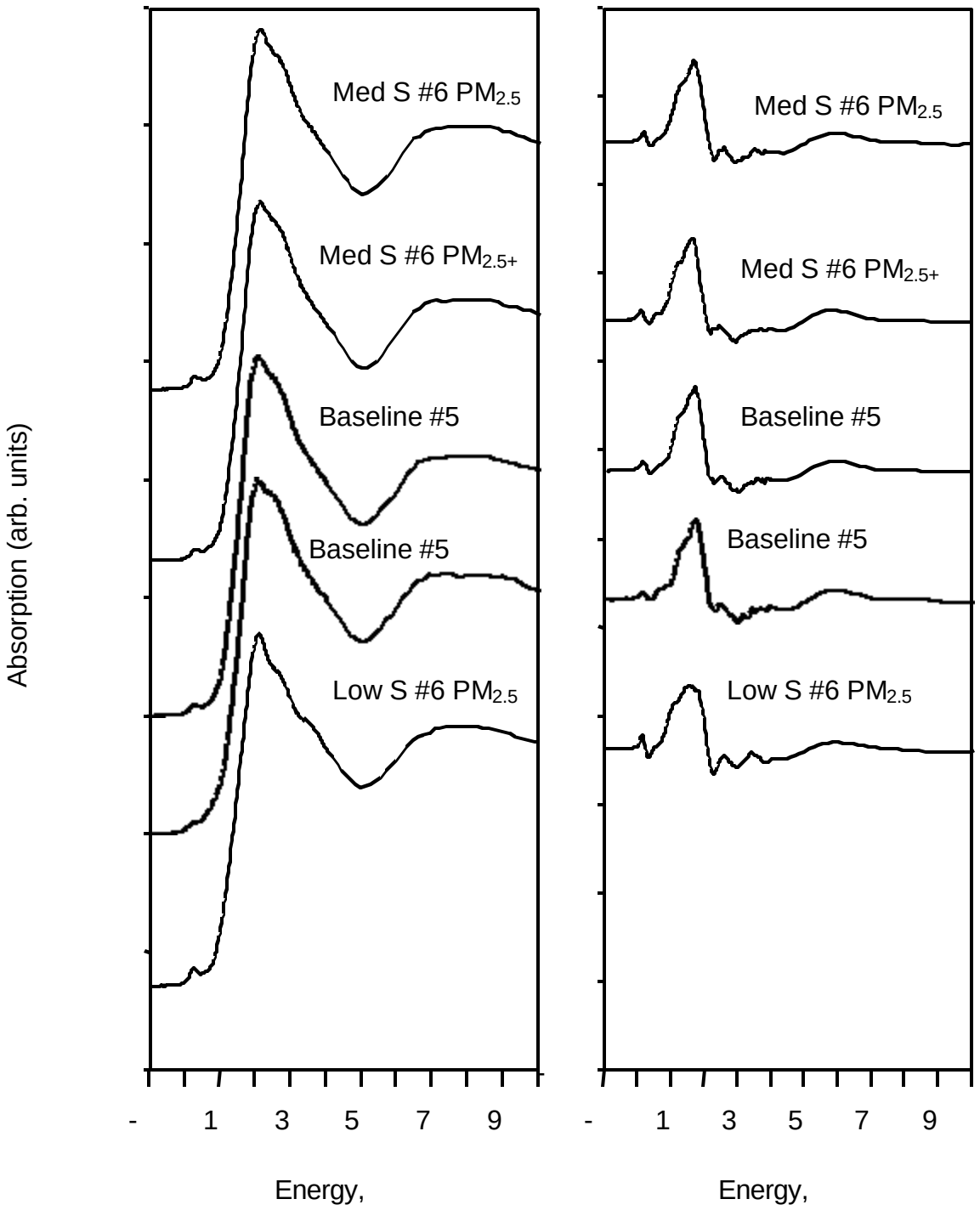

Figure 4. Fe XANES and first derivative spectra indicate that $Fe_2(SO_4)_3$ is the dominant Fe compound in ROFA $PM_{2.5}$. The spectra are normalized to unit step height for easy comparison.

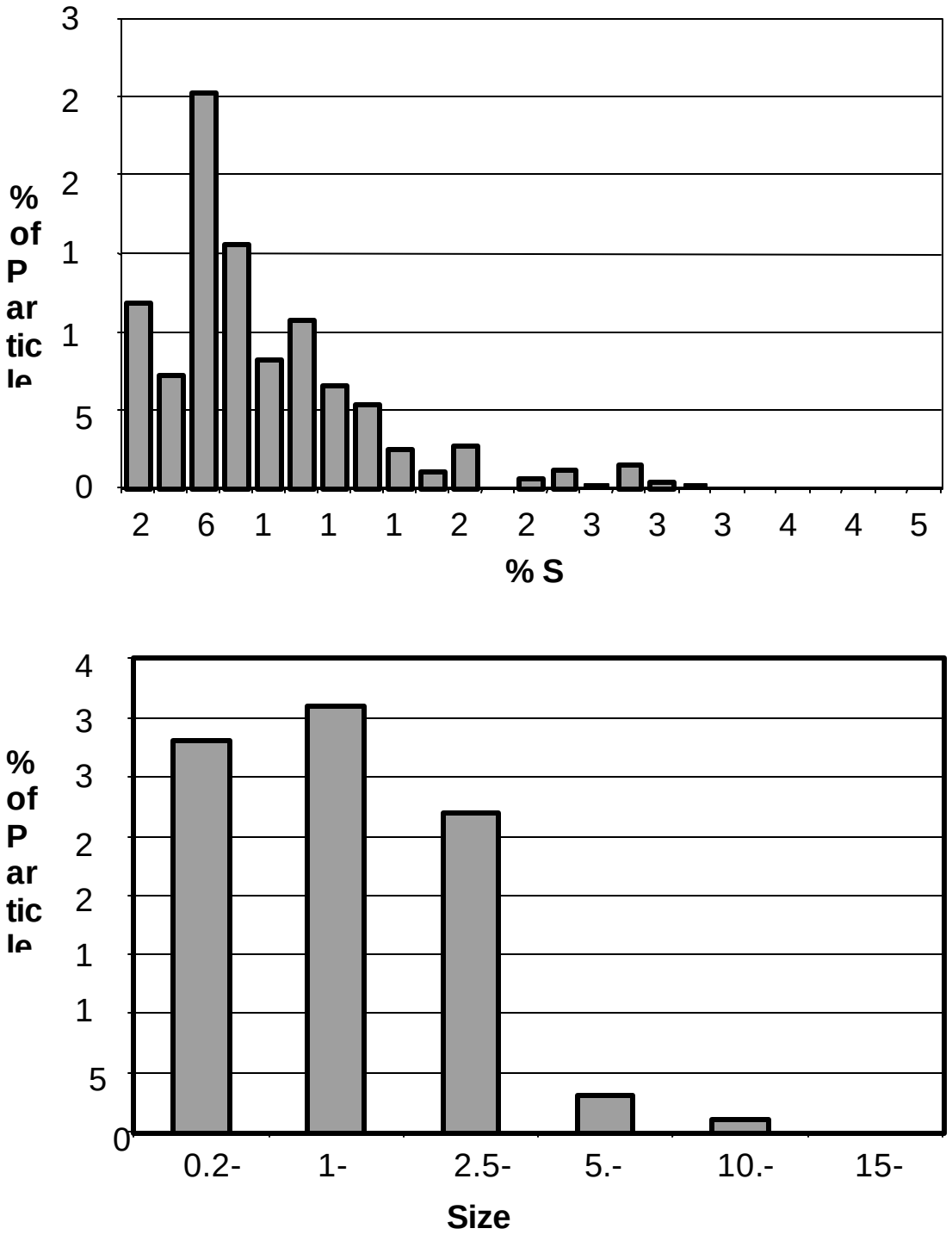

Figure 5. Top – CCSEM C-S distribution for medium S #6 $PM_{2.5}$. Bottom – CCSEM particle size distribution for low S #6 $PM_{2.5}$.

Figure 6. SEM micrographs of highly vesicular carbon-rich char particles. The arrows point to inorganic particles that are rich in V and S.

This file has been forwarded separately as a Powerpoint file.

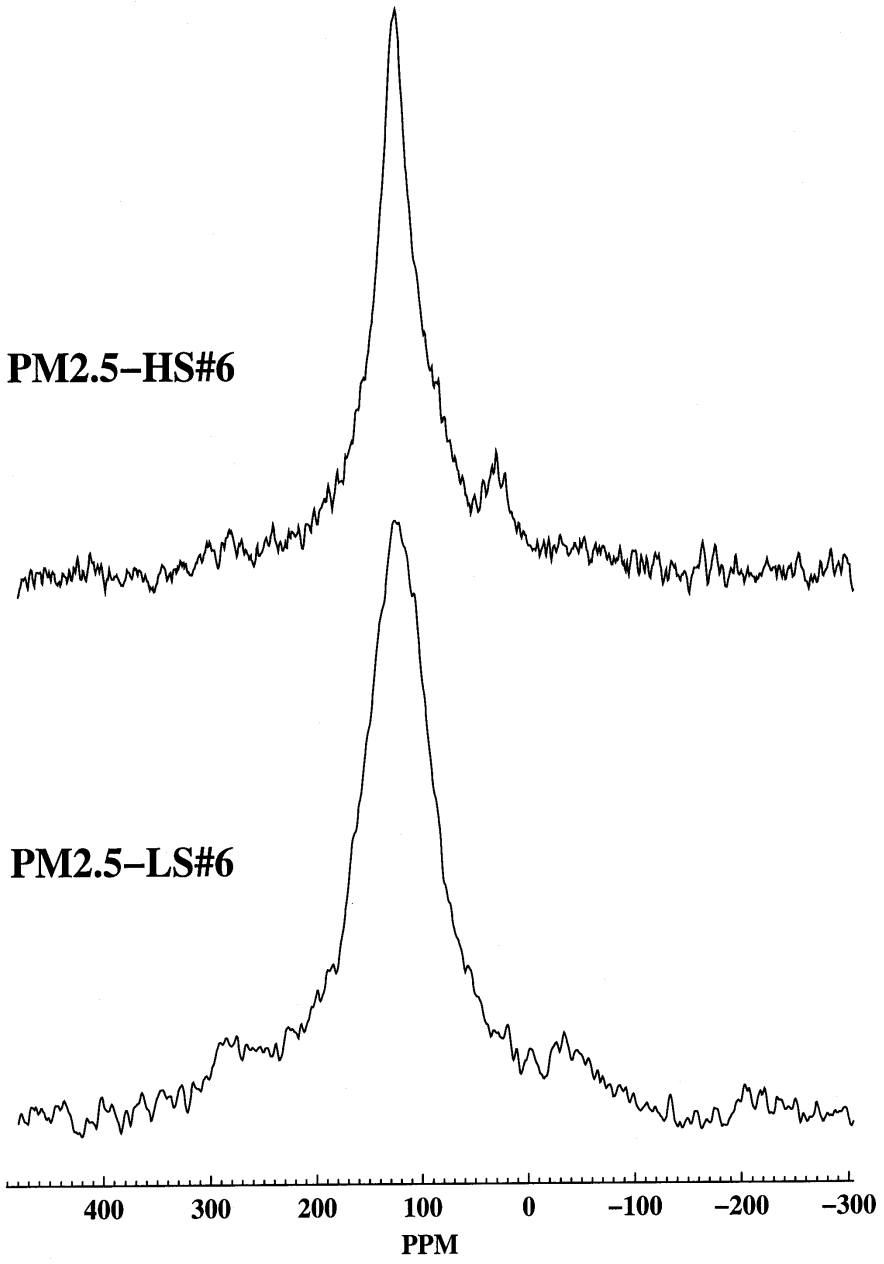

Figure 7. ^{13}C NMR spectra of $PM_{2.5}$ from ROFA. Only the low S #6 $PM_{2.5}$ sample shows any aliphatic structure (top spectrum).

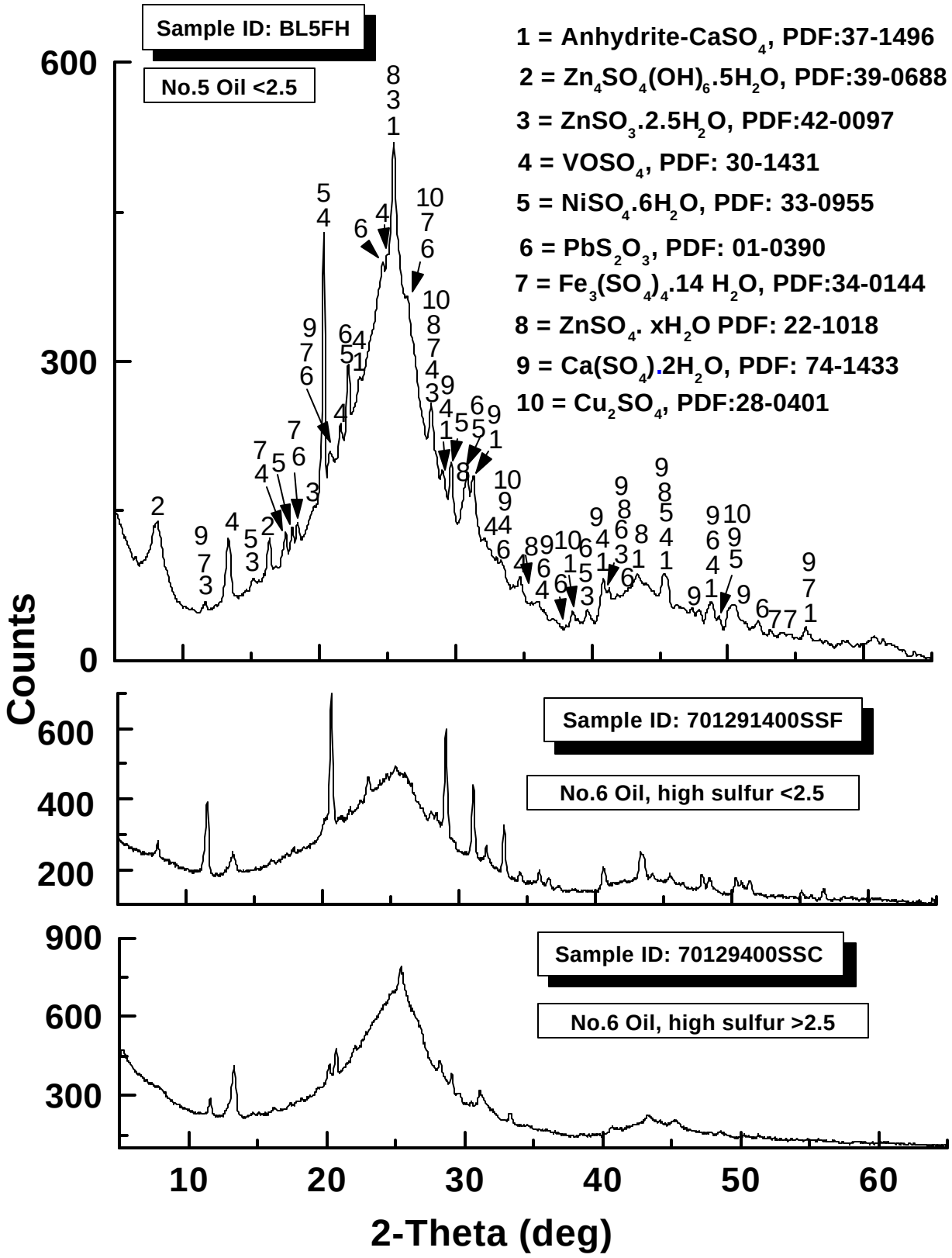

Figure 8. Typical x-ray diffractograms of PM2.5 and PM2.5+ samples from ROFA.